A Narrowband Metamaterial Absorber for Molecular Spectroscopy

Milad Salek[1], and Kaveh Pasandideh[1*]

[1]Department of Engineering Physics, Faculty of Sciences, Kermanshah University of Technology, Kermanshah, Iran

Received: 2026-02-21 Final revised: 2026-06-21 Accepted: 2026-09-20

Abstract

This research focuses on the analysis of a metal-dielectric-metal structured metamaterial absorber aimed at achieving resonant absorption with an ultra-narrow spectral bandwidth in the mid-infrared region. The initial evaluation of the structure's electromagnetic response was carried out through full-wave electromagnetic simulations using CST Studio Suite. To enhance the design efficiency, an equivalent circuit model was developed, enabling the extraction of effective structural parameters and rapid evaluation of its resonant behavior. A parametric sensitivity analysis based on this model quantitatively determined the influence of geometric variables on key absorption characteristics, including the resonance wavelength location, peak absorption, and Full Width at Half Maximum. Optimization results indicate that this absorber is capable of achieving perfect absorption with a very narrow bandwidth; for instance, at the resonant wavelength of $7.89\ \mu m$, an absorption of approximately 99.99% with a bandwidth of about $0.67\ \mu m$ was observed. The demonstrated narrowband absorption characteristics make this metamaterial absorber a promising platform for future infrared spectroscopy applications, including bio-chemical sensing systems.

Keywords: Metamaterial; Resonant Absorption; Bandwidth; Equivalent Circuit; Spectroscopy.

[*] k.pasandideh@kut.ac.ir

1. Introduction

Metamaterial absorbers, as a new generation of engineered materials, play a pivotal role in advancing sensing and detection technologies [1, 2]. These nanostructures, with their unique ability to engineer the interaction of light and matter, enable the achievement of desired optical properties [1]. The ability to design absorbers with narrow bandwidths and near-perfect absorption for infrared spectroscopy significantly increases the practical relevance of these structures [3]. These capabilities, along with the advantages of miniaturization and cost reduction, have made them essential components for the development of the next generation of infrared sensors in the fields of medicine, environmental monitoring, and chemical detection [4].

Metal-Insulator-Metal (MIM) infrared metamaterial absorbers consist of a three-layer structure including a top metal layer with a periodic array of patterned nanostructures, a thin insulator layer in the middle, and a continuous metal plate at the bottom. In this configuration, the nanostructures in the top layer selectively excite surface plasmon resonance at the desired infrared wavelengths. This resonance strongly confines the electromagnetic field within the insulator layer and maximizes energy dissipation. This design simultaneously provides near-unity absorption and precise tunability of the resonance wavelength [5].

Various patterns have been proposed for tuning the resonance wavelength in these structures. Array patterns composed of square or circular patches are among the first and simplest designs that have been used [5]. These patterns are capable of creating strong absorption resonances but typically have a relatively broad absorption bandwidth. The use of parallel arrays of nanowires can lead to the creation of polarization-sensitive absorbers [6]. Split-ring resonators, originally developed for microwave applications and later extended to plasmonic structures, can also create strong magnetic resonances and be used for absorber applications [7]. Meta surfaces consisting of nano-disk arrays are also used to create near-perfect absorbers in the visible region [8]. Furthermore, cross-shaped nanostructures are insensitive to the polarization and angle of incidence of light due to their symmetry [5, 9]. This feature is highly desirable for practical applications such as chemical sensors, where the orientation of target molecules may be random.

The mid-infrared region (i.e., 3- 12 micrometers) is critical for sensing applications due to the presence of unique molecular absorption lines of gases and organic materials [10]. The selective and accurate detection of various gases in the environment requires sensors capable of operating at specific wavelengths with high spectral precision. Achieving this precision necessitates the design of absorbers with very narrow bandwidths. Another significant challenge in gas detection systems is the need for a tunable absorption wavelength, enabling a single absorber to be used for detecting multiple gas types at different wavelengths or to compensate for environmental fluctuations [10].

Extensive research has been conducted on designing high-quality factor metamaterial absorbers for this purpose, with much of it focused on the terahertz range [11-14]. For example, in 2019, a structure comprising a dielectric-patterned meta surface with periodic cross-shaped patterns on a metallic reflector layer was investigated. Results showed that this structure is a perfect absorber with a narrow bandwidth around 7 micrometers [15]. Also, combined patterns such as circular and square rings [11] and metallic strips with

complex configurations [14] have demonstrated their potential for tuning the structure's response.

To introduce dynamic tunability into absorbers, graphene has emerged as an attractive material. Due to its ability to tune its Fermi level through an applied external voltage, graphene is considered an ideal material for the dynamic and electronic control of the optical response of plasmonic absorbers [16]. For example, in 2021, it was shown how a graphene-based plasmonic metamaterial absorber could be used for gas detection in the infrared region [17]. This approach, along with other work in the terahertz range focusing on tunability and reconfiguration [12], paved the way for developing advanced sensors in the mid-infrared region.

In this paper, the simulation and analysis of a metamaterial absorber's behavior in the mid-infrared region are performed. The core objective of this research is to design an optimized metamaterial absorber that can simultaneously achieve near-perfect absorption, a very narrow absorption bandwidth (for high spectral accuracy), and tunability within the 4- 9 micrometer wavelength range. Furthermore, to expedite the parameter optimization process and reduce the computational cost of simulations, a compact RLC equivalent circuit for modeling the system's resonant response is implemented.

2 .Theory and Methodology

2.1 Geometry of the Metamaterial Absorber

Figure 1 shows the structure of a unit cell of the metamaterial absorber. The unit cell is periodically repeated along both the x and y directions. As shown, the ground layer is made of gold with a thickness of d_{au} and the insulator dielectric layer with a thickness of d_{sl}. The top layer is a meta surface with a cross-shaped pattern, where the arm width and length are a and b, respectively. Aligned with this research's objective, this layer is also made of gold, and its thickness is set equal to that of the ground layer. The pattern periodicity is defined by T. The chosen geometry ensures independence from the polarization and angle of the incident light.

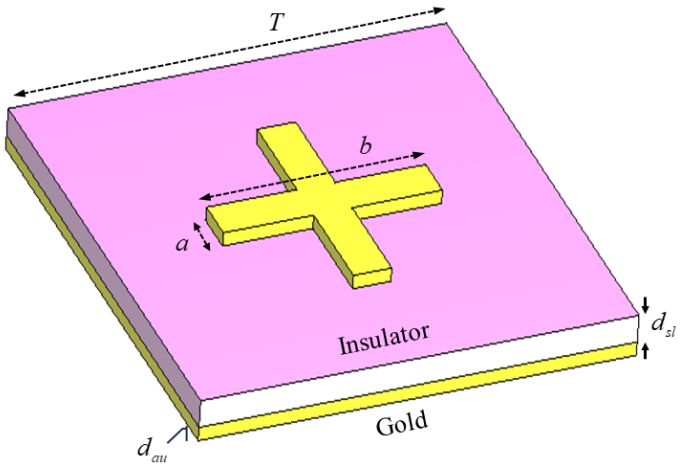


Fig. 1. Structure of a unit cell of metamaterial absorber for operation in the mid-infrared region.

2.2 Modeling and Simulation Analysis

CST Studio Suite software is used to evaluate the performance of the introduced structure. It should be noted that CST is one of the reputable software packages for numerical analysis of electromagnetic phenomena in nanostructures in the high-frequency range, and its results, in terms of accuracy and reliability compared to experimental data, have been widely validated by the research community [18-20].

For analyzing the electromagnetic response of complex structures such as metamaterials or high-frequency circuits, an equivalent circuit model is also used. This approach provides an analytical simplification of the problem. In this model, by mapping electromagnetic field effects such as energy storage and losses to standard circuit elements like capacitors, inductors, and resistors, the influence of geometric and environmental parameters on the structure's frequency response can be intuitively extracted and predicted without the need to fully solve Maxwell's equations [11, 12]. This model not only validates the numerical simulations but also facilitates rapid design optimization.

The equivalent circuit model of this structure, Figure 2, is an RLC circuit where different components model distinct electromagnetic properties.

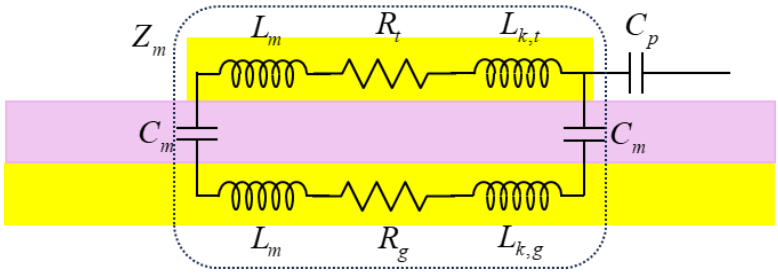


Fig. 2. Equivalent circuit model of the metamaterial absorber.

The circuit consists of a coupling capacitor C_p in series with an RLC branch. The coupling capacitor models the coupling between adjacent cells (electric dipole resonance), and the second section models the magnetic dipole resonance [21]. The inductance and capacitance between two metal layers (L_m, C_m) and coupling capacitor are obtained as follows:

$$C_p = \frac{\pi \varepsilon_0 a}{\ln\left(\frac{2(T-b)}{d_{au}} + \sqrt{\left(\frac{2(T-b)}{d_{au}}\right)^2 - 1}\right)} \tag{1}$$

$$C_m = c\,\varepsilon_0\,\varepsilon_{sl}\,\frac{b}{2}\,\frac{a}{d_{sl}} \tag{2}$$

$$L_m = \frac{1}{2}\,\mu_0\,d_{sl}\,\frac{b}{a} \tag{3}$$

In the above equations, $\mu_0 = 4\pi \times 10^{-7}\ H\ m^{-1}$ represents the permeability of free space and $\varepsilon_0 = 8.85 \times 10^{-12}\ F\ m^{-1}$ represents the permittivity of free space. The relative permittivity of the insulator layer is denoted by ε_{sl}. In Relation (2), the parameter c is introduced to account for the effect of non-uniform field distribution at the surface when calculating the mutual capacitance. According to simulation results, its value lies between 0.4 and 0.55.

The Kinetic Inductance L_k and Resistance R, stemming from the imaginary and real components of gold's impedance, serve to model energy storage and dissipation, respectively, within the Drude formalism. Notably, the magnitudes of these parameters exhibit variance depending on the geometry, specifically, they differ between the cross-shaped nanostructure and the underlying ground layer.

$$L_{k,t} = \frac{c'b}{a\,\delta_{au}} \frac{1}{\varepsilon_0\,\omega_p^2}, \quad R_t = \frac{c'b}{a\,\delta_{au}} \frac{1}{\sigma_{au}} \tag{4}$$

$$L_{k,g} = \frac{2}{\delta_{au}} \frac{1}{\varepsilon_0\,\omega_p^2}, \quad R_g = \frac{2}{\delta_{au}} \frac{1}{\sigma_{au}} \tag{5}$$

In the preceding equations, $\omega_p = 13.6\times10^{15}\ rad/s$ is the angular plasma frequency of gold. The penetration depth is described by the relation $\delta_{au} = \lambda / 2\pi\kappa$, where κ is the extinction coefficient of gold. The DC conductivity of gold is characterized by $\sigma_{au} = \varepsilon_0\,\omega_p^2\,\tau_{au}$, where $\tau_{au} = 12.4\times10^{-15}\,s$ is the relaxation time. In equation (4), the numerical parameter $c' \approx 0.6$ is introduced specifically to account for the effect of non-uniform current distribution on the surface in the calculations.

The absorption of the structure is calculated by employing Transmission Line Theory. Utilizing the provided equivalent circuit model, the total input impedance to the line is expressed as $Z_s = Z_e + Z_m$, where $Z_e = (2\pi i f\, C_p)^{-1}$ represents the impedance arising from the coupling capacitor, and Z_m pertains to the RLC circuit, which can be calculated as follows:

$$Z_m = \frac{(2\pi i f)^3 C_m L_t L_g + (2\pi i f)^2 C_m (L_t R_g + L_g R_t) + (2\pi i f)(C_m R_t R_g + 2L_t) + 2R_c}{2 + (2\pi i f)^2 C_m (L_t + L_g) + (2\pi i f) C_m (R_g + R_t)} \tag{6}$$

In deriving this relationship, we have utilized $L_{t,g} = L_m + L_{k,(t,g)}$ for further simplification. Within this model, the reflection coefficient is given by the following relation:

$$\Gamma_{in} = \frac{Z_s - Z_0}{Z_s + Z_0} \tag{7}$$

Where $Z_0 = \sqrt{\mu_0 / \varepsilon_0} \approx 377\ \Omega$ is the impedance of free space. Subsequently, the absorption coefficient will be obtained using the relationship $A = 1 - |\Gamma_{in}|^2$.

3 . Results and Discussion

The absorber was simulated using CST Studio Suite. To ensure numerical accuracy, the simulations were performed in the frequency domain. Given the periodic structure of the absorber, the Floquet Port was utilized to impose periodic boundary conditions. The data corresponding to the permittivity of gold and the insulator were extracted from Refs [22] and [23], respectively.

Figure 3 illustrates the absorption spectrum of the absorber as a function of wavelength with a silica (SiO_2) insulator layer. The values of the parameters used in the simulation are listed within the figure itself. At the resonance wavelength of $\lambda_{res} = 6.25\,\mu m$, the

absorption coefficient reaches approximately 99.63%. Furthermore, the absorption bandwidth is $0.36\,\mu m$. It is noteworthy that this narrow bandwidth is considered highly desirable for spectroscopic applications in the infrared region.

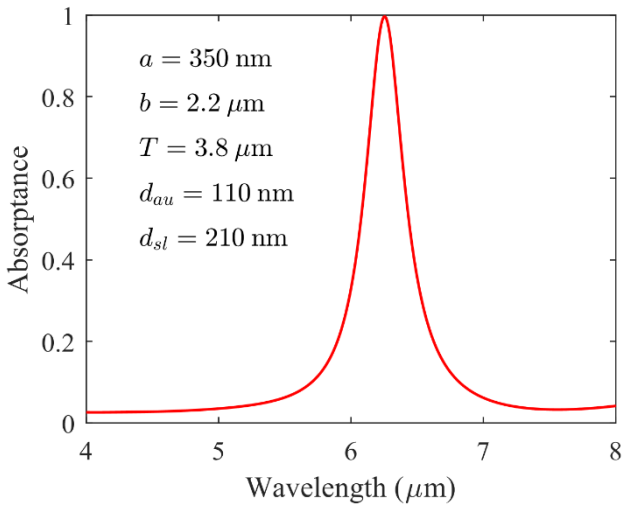


Fig. 3. Absorption coefficient of the metamaterial absorber as a function of wavelength.

Figure 4 shows the electric field intensity distribution near the cross-shaped nanostructure at the resonance wavelength. The maximum electric field intensity is observed at the edges of the gold cross-shaped nanostructure, which signifies the excitation of the localized surface plasmon resonance and the intense field confinement within the silica layer. The localized and symmetric field distribution indicates the excitation of the dipole mode within the structure.

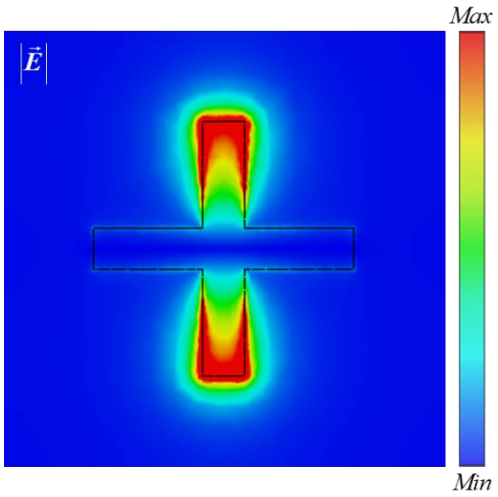


Fig. 4. Electric field Intensity distribution on the absorber surface at the resonance wavelength of 6.25 μm.

Direct optimization of the structural parameters using full-wave simulations imposes a significant computational burden. Therefore, we analyzed the response of the designed absorber using the equivalent circuit model. To verify the validity of this model, simulations were initially performed using identical parameter values in both the software and the equivalent circuit model, and the resulting comparison is presented in Figure 5. The parameter values used in the analysis included a gold thickness of $100\,nm$, a silica

thickness of $200\,nm$, and a structural periodicity of $3.5\,\mu m$. Moreover, the arm width and length of the cross-shaped top nanostructure were set to $400\,nm$ and $1.8\,\mu m$, respectively.

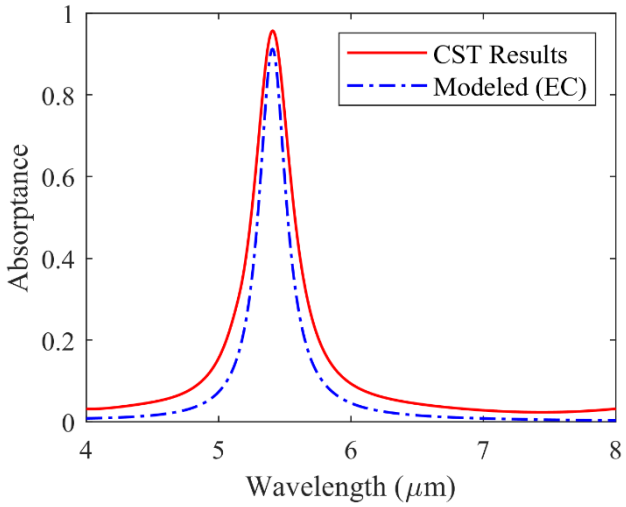


Fig. 5. Comparison of absorption spectrum between Equivalent Circuit model and CST Simulation results.

The results indicate that the equivalent circuit model successfully reproduces the data obtained from the full-wave simulations with acceptable accuracy. Therefore, this model can be confidently employed for the optimization of geometric parameters to achieve the desired absorption response while significantly reducing both computational and time costs. Using this model, a series of simulations were performed to extract the dependence of the resonance wavelength, resonance bandwidth, and absorption coefficient on the key structural parameters. The main findings derived from these analyses are discussed in the following sections.

Figure 6 illustrates how the resonance wavelength and maximum absorptance are dependent on the arm length b . The simulations utilized a fixed periodicity of $3.5\,\mu m$ and an arm width of $350\,nm$.

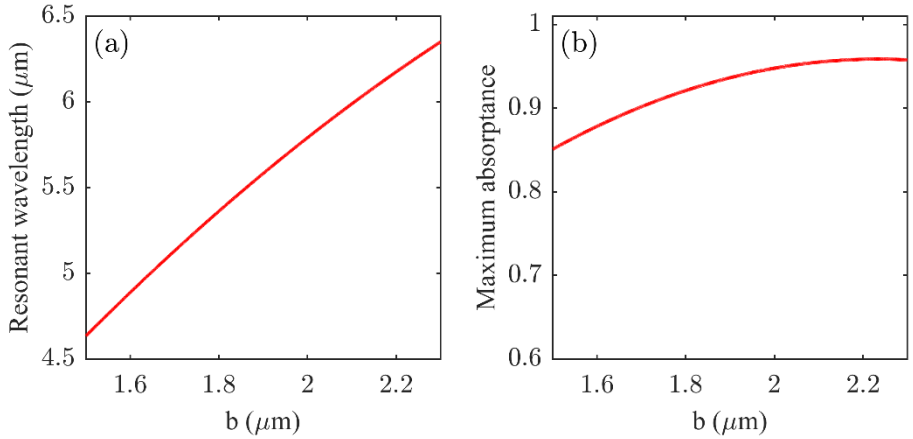


Fig. 6. Dependence of a) resonance wavelength and b) maximum absorptance coefficient on the arm length. The results were obtained using the equivalent circuit model.

Within the simulation range, this parameter showed no significant effect on the maximum absorptance and absorption bandwidth. However, it is observed that the

resonance wavelength has a direct and significant dependence on this parameter. By varying the arm length from 1.5 to $2.3\,\mu m$, the resonance wavelength shifts within the $4.6-6.3\,\mu m$ range. This dependence can be explained using Eq. (6). To obtain the resonance wavelength, the imaginary part of the effective impedance Z_s must be set to zero. By doing so, we arrive at the following relation:

$$\lambda_{res} \propto \sqrt{C_m \left(L_g + L_t\right)} \propto b$$

In accordance with this relationship, the arm length has a direct relationship with the resonance wavelength, which justifies the results presented in Figure 6(a). Increasing the structure's periodicity up to $6\,\mu m$ had a negligible effect on the resonance wavelength. Therefore, this parameter can be utilized to fine-tune the structure's response for the intended application. Notably, several gases, including CO, N_2O, and NO possess absorption lines within this spectral range.

Simulation data further indicate that the periodicity and the arm width primarily affect the absorption bandwidth, as shown in Figure 7. The figure illustrates the dependence of the absorption width and the maximum absorption on the arm width for several different values of the periodicity. In this series of simulations, the thickness and length of the top nanostructures were set to $100\,nm$ and $2.2\,\mu m$, respectively, and the insulator thickness was considered to be $200\,nm$. The resonance wavelength in this case was approximately $6.25\,\mu m$ and exhibited only slight variations.

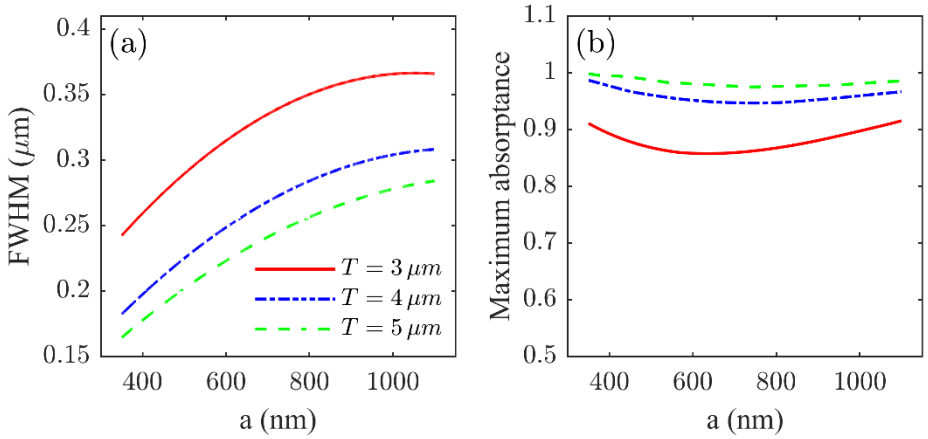


Fig. 7. a) Dependence of the absorption bandwidth, and b) maximum absorptance coefficient on the arm width of the top cross-shaped nanostructure.

According to Eq.6, the FWHM of the absorption curve is proportional to $a / Ln(T)$. For a fixed periodicity, an increase in arm width corresponds to an increase in the absorption bandwidth, as clearly observed in Figure 7(a). Furthermore, increasing the structure periodicity and decreasing the coupling between adjacent cells leads to a narrower absorption peak.

To extend the absorption towards longer wavelengths, an aluminum nitride (AlN) insulator layer was integrated into the structure. AlN's exceptional thermal conductivity and favorable dielectric characteristics render it a compelling candidate for infrared sensing applications [23]. Initially, the equivalent circuit model was utilized to optimize the parameters of the structure for near-complete absorption. Subsequently, simulations were conducted using these optimized parameters in the software. Table 1 presents

simulation outcomes derived from CST software, detailing the resonance wavelength (λ_{res}) and maximum absorptance coefficient ($A_{\max}$). These simulations were performed using an arm width of $200\,nm$, gold layer thickness of $150\,nm$, insulator thickness of $250\,nm$, and an arm length spanning from 1.7 to $2.5\,\mu m$. The data unequivocally demonstrate a red-shift in resonance to longer wavelengths when employing AlN as the insulator, in contrast to silica. This observed red-shift is explicable by AlN's higher dielectric constant relative to silica, which augments the inter-layer capacitance. Consequently, a pronounced red-shift in the resonance wavelength is realized.

Table 1. Resonance wavelength and maximum absorptance coefficient values for the metamaterial absorber with AlN insulator, arm width of $200\,nm$, and for two different structure periodicity values.

$b\,(\mu m)$	$T = 2.8\,\mu m$		$T = 3.2\,\mu m$	
	$A_{\max}(\%)$	$\lambda_{res}\,(\mu m)$	$A_{\max}(\%)$	$\lambda_{res}\,(\mu m)$
1.7	99.24	6.80	99.68	6.85
1.8	99.65	7.10	99.27	7.20
1.9	99.92	7.41	98.79	7.47
2.0	99.98	7.71	98.31	7.71
2.1	99.99	7.89	98.05	7.91
2.2	99.95	8.12	98.04	8.07
2.3	99.62	8.40	97.11	8.33
2.4	98.04	8.84	93.75	8.73
2.5	97.11	9.03	92.12	8.93

A remarkable finding is the near-perfect absorption of 99.99% at a wavelength of $7.89\,\mu m$, achieved with a structure periodicity of $2.8\,\mu m$ and arm length of $2.1\,\mu m$.

This high level of absorptance indicates the significant potential and effectiveness of the design investigated in this study as a complete absorber in the mid-infrared region. It may have extensive applications in areas such as infrared spectroscopy, infrared imaging, and advanced optical sensors. Given its operational range and narrow bandwidth, the examined metamaterial absorber provides a promising platform for future infrared spectroscopy and sensing applications, where its selective absorption characteristics may be utilized for the detection of molecular signatures of gases such as HF, H_2S, and ammonia.

Notably, this absorber was compared with recently reported mid-infrared metamaterial absorbers based on similar MIM configurations. As reported in [16], the authors developed an Au/graphene/AlN absorber, where the resonance response was tuned by graphene chemical potential, while the geometrical parameters, particularly the resonator length, controlled the resonance wavelength. Similarly, our results confirm the important role of resonator dimensions in controlling the absorption response. Compared with graphene-based absorbers, the proposed structure achieves narrowband near-perfect absorption through geometrical optimization without requiring an active tuning mechanism. The AlN-based dual-band absorber reported in [9] also demonstrated selective infrared absorption using a graphene-integrated structure. However, its spectral tunability relies on graphene modulation, whereas the present design focuses on a simpler single-band narrow absorption response.

4. Conclusion

In this research, a Metal-Insulator-Metal (MIM) metamaterial absorber was investigated. The top layer consisted of a periodic array of gold cross-shaped nanostructures, which ensures that the absorption characteristics are independent of the incident wave's polarization and angle of incidence. In the absorber's design, two types of insulators, Silica (SiO_2) and Aluminum Nitride (AlN), were used to study the effect of the material type on the absorption properties.

Initially, CST simulations demonstrated that near-perfect absorption could be achieved by appropriately tuning the structural dimensions. For more detailed analysis and structural optimization, an equivalent circuit model was employed. This model accounted for the effects of coupling between adjacent cells and magnetic dipole resonance. Based on this model, the influence of geometric parameters such as the length and width of the top cross-shaped nanostructure and the period on the structure's absorption behavior was examined.

The results indicated that, when silica was used, the resonance wavelength fell within the range of 4-7 micrometers. Crucially, the transition to Aluminum Nitride as the spacer material facilitates a significant redshift of the resonance, pushing it into the $7-9\,\mu m$ spectrum, which is attributable to its higher dielectric constant. Overall, the investigated metamaterial absorber provides a promising platform for future infrared sensing applications owing to its narrow bandwidth and spectral tunability.

5. Declarations Conflict of Interest

The authors declare that they have no known competing financial interests or personal relationships that could have appeared to influence the work reported in this paper.

References

[1] M. Amiri, F. Tofigh, N. Shariati, J. Lipman, M. Abolhasan, Review on metamaterial perfect absorbers and their applications to IoT, IEEE Internet of Things Journal, 8 (2020) 4105-4131.

[2] N.I. Landy, S. Sajuyigbe, J.J. Mock, D.R. Smith, W.J. Padilla, Perfect metamaterial absorber, Physical review letters, 100 (2008) 207402.

[3] K. Li, Y.-S. Lin, Tunable perfect meta-absorber with high sensitivity for refractive index sensing application, Sensing and Bio-Sensing Research, 45 (2024) 100676.

[4] Y. Yao, Z. Liao, Z. Liu, X. Liu, J. Zhou, G. Liu, Z. Yi, J. Wang, Recent progresses on metamaterials for optical absorption and sensing: a review, Journal of Physics D: Applied Physics, 54 (2021) 113002.

[5] N. Liu, M. Mesch, T. Weiss, M. Hentschel, H. Giessen, Infrared Perfect Absorber and Its Application As Plasmonic Sensor, Nano Letters, 10 (2010) 2342-2348.

[6] Y. He, H. Deng, X. Jiao, S. He, J. Gao, X. Yang, Infrared perfect absorber based on nanowire metamaterial cavities, Optics letters, 38 (2013) 1179-1181.

[7] J. Li, J. Chen, D. Yan, F. Fan, K. Chen, K. Zhong, Y. Wang, Z. Tian, D. Xu, A review: Active tunable terahertz metamaterials, Advanced Photonics Research, 5 (2024) 2300351.

[8] X. Wang, H. Lu, B. Wang, M. Liu, G. Guo, S. Ma, J. Lv, J. Liang, W. Wang, Broadband metamaterial absorber based on plasmonic nanodisk array and its application in boosting the performance of photodetector, Optics & Laser Technology, 185 (2025) 112581.

[9] M. Alijabbari, R. Karimzadeh, S. Pakniyat, J.S. Gomez-Diaz, Dual-band and spectrally selective infrared absorbers based on hybrid gold-graphene metasurfaces, Opt. Express, 32 (2024) 16578-16590.

[10] S. Tabassum, S. Nayemuzzaman, M. Kala, A. Kumar Mishra, S.K. Mishra, Metasurfaces for sensing applications: Gas, bio and chemical, Sensors, 22 (2022) 6896.

[11] Z. Lu, P. Li, C. Zhang, S. Li, R. Chen, Z. Zhou, X. Huang, Terahertz metamaterial absorber and equivalent circuit model for refractive index sensing, Materials, 18 (2025) 765.

[12] Shruti, S. Pahadsingh, B. Appasani, A. Srinivasulu, N. Bizon, P. Thounthong, A reconfigurable terahertz metamaterial absorber for gas sensing applications, Crystals, 13 (2023) 158.

[13] A. Teber, Refractive Index Sensor Based on Terahertz Metamaterial Absorber with High Sensitivity and Quality Factor for Sensing Applications, Türk Doğa ve Fen Dergisi, 13 (2024) 61-68.

[14] D. Wang, K.-D. Xu, S. Luo, Y. Cui, L. Zhang, J. Cui, A high Q-factor dual-band terahertz metamaterial absorber and its sensing characteristics, Nanoscale, 15 (2023) 3398-3407.

[15] S. Chen, Z. Chen, J. Liu, J. Cheng, Y. Zhou, L. Xiao, K. Chen, Ultra-narrow band mid-infrared perfect absorber based on hybrid dielectric metasurface, Nanomaterials, 9 (2019) 1350.

[16] M. Alijabbari, R. Karimzadeh, Performance optimization of hybrid gold-graphene metasurface infrared absorbers for dominant single-band response with dynamic resonance shifts, Optical Materials Express, 15 (2025) 425-445.

[17] Y.E. Monfared, M. Qasymeh, Graphene-assisted infrared plasmonic metamaterial absorber for gas detection, Results in Physics, 23 (2021) 103986.

[18] L. Li, F. Chen, Tunable four-band metamaterial absorber and sensor based on a stacking double-ring Dirac semimetal structure design, Physics Letters A, 544 (2025) 130489.

[19] C.M. Studio, CST Microwave studio, 2008.

[20] F. Umaña-Idarraga, D. Cataño-Ochoa, S. Montoya-Villada, C. Valencia-Balvin, E. Reyes-Vera, Design of a perfect and multi-resonant metamaterial absorber for electromagnetic energy harvesting applications, Journal of Physics: Conference Series, IOP Publishing, 2021, pp. 012005.

[21] S. Kang, Z. Qian, V. Rajaram, S.D. Calisgan, A. Alù, M. Rinaldi, Ultra-narrowband metamaterial absorbers for high spectral resolution infrared spectroscopy, Advanced Optical Materials, 7 (2019) 1801236.

[22] A.D. Rakić, A.B. Djurišić, J.M. Elazar, M.L. Majewski, Optical properties of metallic films for vertical-cavity optoelectronic devices, Applied optics, 37 (1998) 5271-5283.

[23] J. Kischkat, S. Peters, B. Gruska, M. Semtsiv, M. Chashnikova, M. Klinkmüller, O. Fedosenko, S. Machulik, A. Aleksandrova, G. Monastyrskyi, Mid-infrared optical properties of thin films of aluminum oxide, titanium dioxide, silicon dioxide, aluminum nitride, and silicon nitride, Applied optics, 51 (2012) 6789-6798.